Mineral and chemical composition of the ores at the Dve Vody Sb-Au deposit, Western Carpathians

JURAJ MAJZLAN[1], MARTIN CHOVAN[2] & JOZEF MICHÁLEK[3]

[1] Department of Geology, University of California at Davis, Davis, CA 95616, USA
[2] Department of Mineralogy and Petrology, Comenius University, Mlynská dolina G, 842 15 Bratislava, Slovakia
[3] EnviGeo, Ltd., Kyncelová 10, 974 01 Banská Bystrica, Slovakia

Abstract. The Hercynian crystalline complex of the Nizke Tatry Mountains (Western Carpathians, Slovakia) hosts a number of hydrothermal ore deposits, variable in their mineral and chemical composition. The Dve Vody deposit is one of them, with several separate vein systems in gneisses and migmatites. The ore samples, collected at waste dumps of the adits, were investigated by the means of optical microscopy, electron microprobe analyses, X-ray diffraction, and bulk analyses for Ag, As, Au, Cu, Pb, Sb, and Zn by a combination of spectroscopic techniques. There are As-Au, Sb, base-metals, and siderite mineralizations developed in the deposit, listed in the order in which they were formed. The As-Au mineralization is represented by fine-grained pyrite-arsenopyrite ores hosted by gray quartz. These ores are the principal gold carrier in the deposit (up to 14 ppm Au). The Sb mineralization comprises three parageneses: carbonate, sulfosalts-sphalerite, and stibnite. Carbonates, varying in their composition from early siderite to late Fe-dolomite, with minor calcite and magnesite, are the earliest paragenesis. Sphalerite is always earlier than the sulfosalts. The most common sulfosalt in the Sb mineralization is zinckenite. Stibnite usually occurs in white quartz or as monomineral veinlets in strongly altered rocks. The principal ore minerals of the base-metals mineralization are galena and pyrite. Silver in these ores appears to be concentrated in infrequent tetrahedrite inclusions in galena. The most abundant minerals of the siderite mineralization are siderite, tetrahedrite, and bournonite. The rock-forming minerals of the wall-rocks, with the exception of quartz, were altered to illite. The investigation of the ore samples was complemented by panning of alluvial sediments. The streams draining the area of the deposit showed elevated concentration of gold flakes (up to 7 gold flakes).

Key words: Nízke Tatry Mts, hydrothermal mineralization, stibnite, gold

Introduction

Nízke Tatry Mts, a mountain ridge in the Western Carpathian arc, is a region with long history of mining of gold, antimony, iron, copper, and other metals (Chovan et al. 1996). Despite the amount of metals extracted, little is known about mineral and chemical composition of the ores. Detailed information on the ores and the rocks that host the ores is necessary to answer the questions of metallogenesis of the region. As a part of our systematic work on the ore deposits in the Nízke Tatry Mts (see also Chovan et al. 1995, Majzlan et al. 1998), we paid attention to one of the larger ore deposits in the region, the deposit Dve Vody. The goal of the presented work is to offer a detailed description of the ore samples from Dve Vody, with emphasis on their mineral and chemical composition. The Dve Vody deposit is compared to other ore deposits in the Nízke Tatry Mts.

Geologic settings

The deposit Dve Vody is located on southern slopes of the Nízke Tatry Mountains, in Stellerova dolina valley, appr. 7 km north from the village of Dolná Lehota. The valley exposes crystalline rocks of the Tatric unit (Biely & Bezák, 1997), dominated by gneisses and migmatites with small amphibolite bodies (Fig. 1). Petrogenetic and regional geological problems of the metamorphosed crystalline rocks were addressed by Janák et al. (1993), Hovorka et al. (1994), Petrík et al. (1998) and others.

History of ore exploitation and research on the Dve Vody deposit is briefly summarized by Michálek (1999). Results of a detailed mineralogical study of the Dve Vody ores were reported by Hak (1966). In addition to the minerals detected in the present study, he found scarce antimony, chalcostibite, jamesonite, and unidentified gold tellurides. We have also not found cinnabar inclusions in stibnite reported by Cambel et al. (1976). Kantor (1948) gives an analysis of the ores of siderite-tetrahedrite veins as Sb 7.96 %, As 0.53 %, Pb 5.57 %, Au 1.4 ppm, Ag 471.6 ppm, Fe 9.26 %, and Cu 3.99 %. Michálek (1993) determined the average metal concentration of the Dve Vody ores from are 3.8 % Sb, 0.4 % As, 4.2 ppm Au, and 3.5 ppm Ag. Munde (1944 in Michálek, 1999) analyzed the Sb-Au ores of the Main vein in the adits 1 and 2 to find Sb 4.48 %, As 0.27 %, 9.08 ppm Au, 11.57 ppm Ag at average vein thickness of 0.70 m. Metalometric prospecting activities (Gubač, 1980) detected an antimony
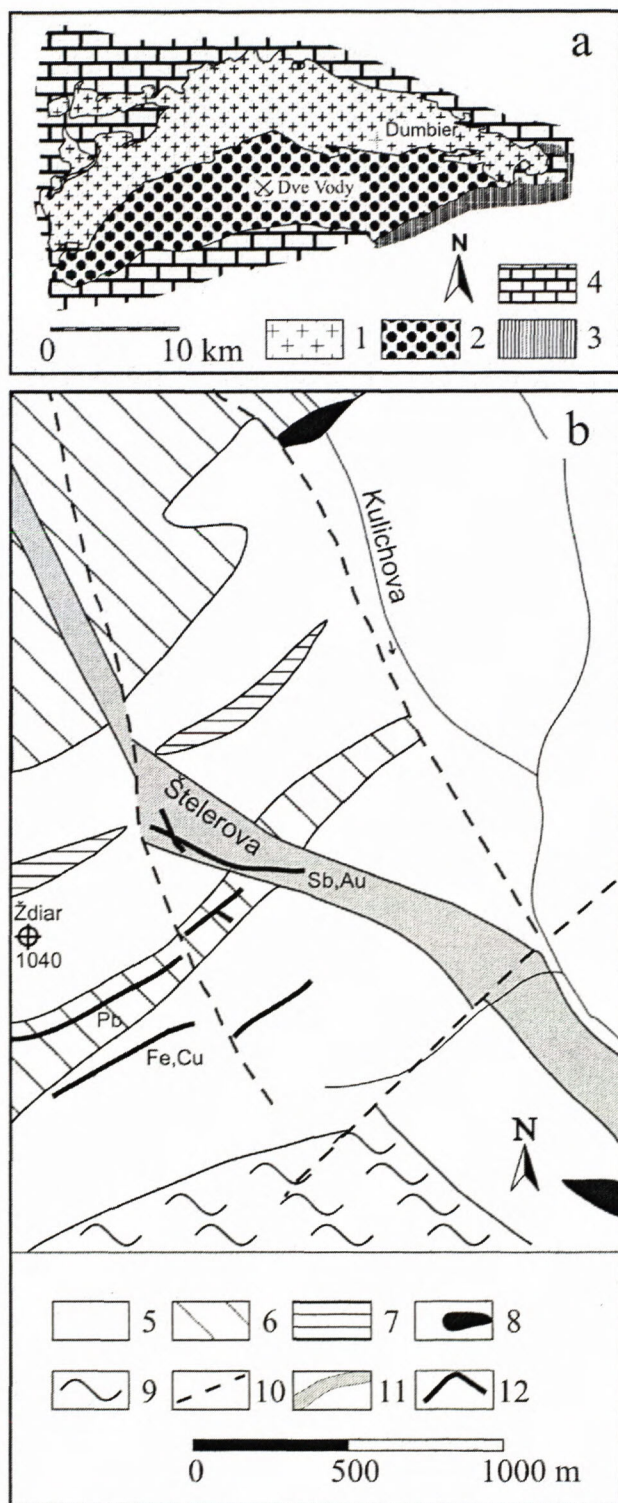
Fig. 1. a) a schematic geologic map of the Ďumbier part of the Nízke Tatry Mts with localization of the Dve Vody deposit, 1 – granitoid rocks of Tatric unit, 2 – high-grade metamorphic rocks of Tatric unit, 3 – Mesozoic sedimentary sequences of Tatric, Veporic, and Hronic unit, 4 – low-grade metamorphic rocks of Veporic unit, b) schematic geologic map of the Dve Vody deposit and vicinity, 5 – biotite – two-mica banded gneisses, 6 – biotite – two-mica ophtalmitic gneisses, 7 – metasediments and metavolcanoclastic rocks with subgraphitic admixture, 8 - amphibolites, 9 – orthogneisses of the Struhár type, 10 – faults, 11 – zones with As-Au and Sb ores, 12 – ore veins.

anomaly northward from the deposit, in the Kulichova dolina valley. Pulec et al. (1983) evaluated the composition of heavy mineral concentrates from the streams in the southern part of the Nizke Tatry Mountains, including the area of the Dve Vody deposit.

The paragenetic studies of the deposit are limited to the work of Kantor (1948) and Hak (1966). Figure 2 reproduces the unpublished paragenetic sequence of Kantor (1948). Hak (1966) distinguished the principal ore formation stages of ore deposits in the Nízke Tatry Mts. The general features of his work are re-iterated in the latest metallogenetic classification of the ores in the Nízke Tatry Mts (Chovan et al. 1996).

(Kantor 1948)

	1	2	3	4
quartz	—	—		
arsenopyrite		—		
pyrite		—		—
sphalerite	-			
ankerite		—		
stibnite		—	—	—
boulangerite				—
calcite				—

Fig. 2. Paragenetic sequence of the Dve Vody deposit after Kantor (1948).

Methods and material

The samples of ore minerals and altered rocks were collected at waste dumps and in the entrance portion of the accesible adits. Sampling of the dumps was accompanied by panning of the stream sediments and the material from selected dumps. The heavy minerals were concentrated from 10-15 kg of sandy (<3 mm) material. In the laboratory, the concentrates were dried and separated to fractions >0.5 mm, 0.2-0.5 mm, and <0.2 mm by sieving. The fraction >0.5 mm usually represented a negligible portion of the concentrate and was not evaluated further. The concentrates were checked for the presence of scheelite with a UV lamp. Cassiterite and wolframite were identified by coloring tests in hot dilute HCl (1:1) and hot aqua regia, respectively. The reported number of gold grains represents a sum for the fraction <0.2 mm and 0.2 – 0.5 mm. Cassiterite, scheelite, wolframite and cinnabar grains were counted only in fraction 0.2 – 0.5 mm.

Thin and polished sections were studied in reflected and transmitted light. All collected bulk samples were checked for the presence of scheelite with a UV lamp. Chemical analyses of the samples were carried out by a combination of atomic absorption spectroscopy techniques for Au (detection limit 0.02 ppm), Ag (0.4 ppm), Cu (0.001 wt.%), Zn (0.001 wt.%), Bi (0.0008 wt.%) in the laboratories of Geologický Prieskum (Geological Survey), Turčianske Teplice, Slovakia. The samples with gold concentration >5 ppm were re-analyzed for gold. The reproducibility of the analyses was inspected on selected samples in the laboratories of Westore Engineering

gold (<5 grains)
(6 - 20 grains)
(50 - 250 grain)
scheelite (<10 grains)
cassiterite (10 - 25 grains)
wolframite (<5 grains)
cinnabar (<5 grains)

elevation point
adit (As-Au and Sb mineralization)
adit (base-metals mineralization)
adit (siderite mineralization)
site of heavy mineral concentrate collection
ST-3 heavy mineral concentrate from alluvial sediments
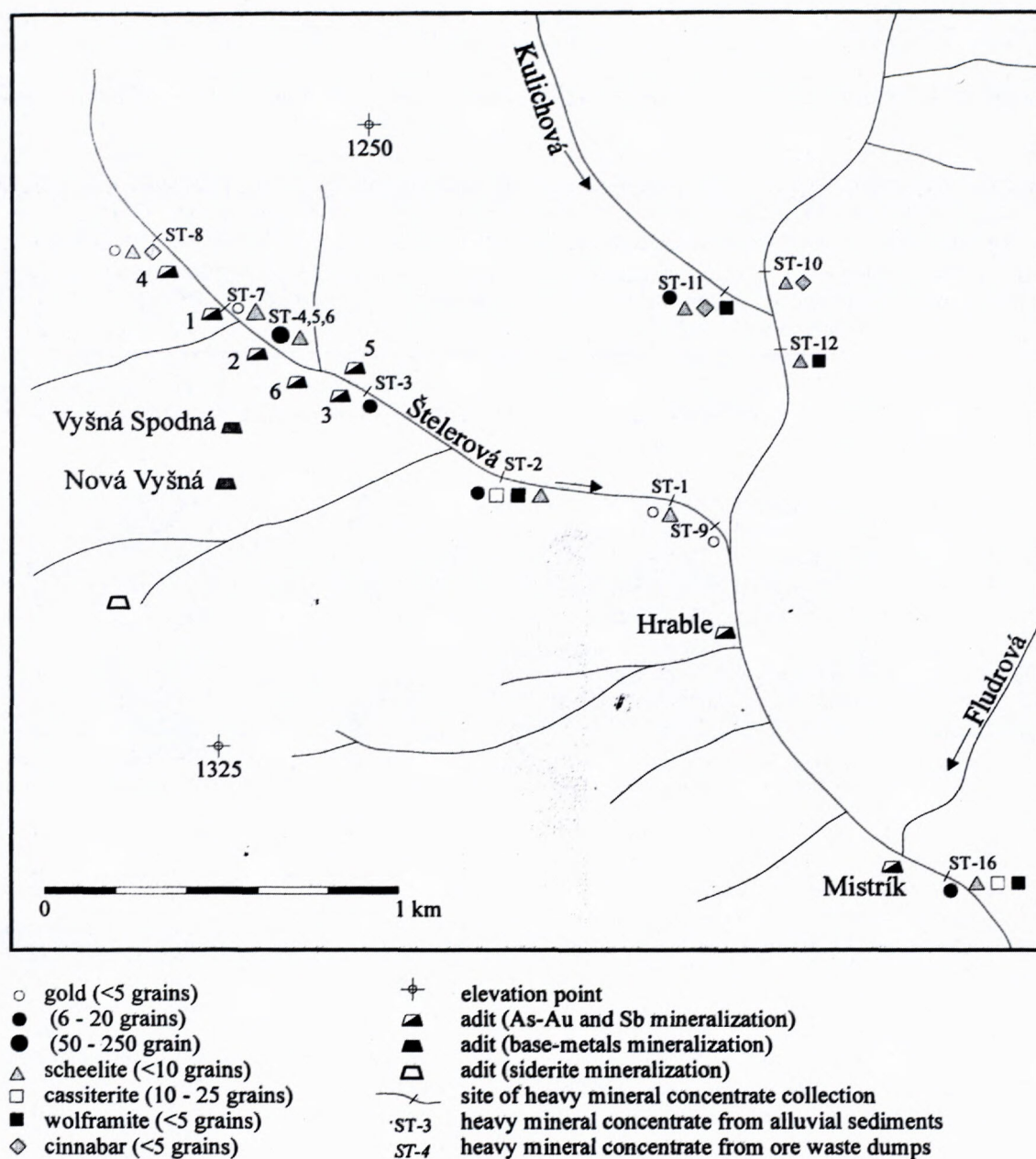ST-4 heavy mineral concentrate from ore waste dumps

Fig. 3. Location of the adits of the Dve Vody deposit and results of panning.

Table 1. A comparison of chemical analyses of bulk ores as analyzed by Geologický Prieskum (Geological Survey), Turčianske Teplice, Slovakia (first entry) vs. Westore Engineering Ltd., Vancouver, Canada (second entry).

	Au	Ag	As	Pb	Sb	Zn	Cu
V-1	17.0/7.5	14.4/9.6	1367/600	4497/3700	3085/2440	59/50	447/300
V-7		15.0/5.2	5969/4300	3534/1270	3643/1300	173/50	67/20
V-10	5.51/7.2	1.1/0.4	759/2000	58/90	23212/10800	109/60	32/10
V-15		7.5/8.0	1901/1900	229/200	517/550	57/80	221/200
V-19	9.70/9.40	1.2/1.2	23116/20800	172/210	269/1040	36/30	25/10
V-20		6.9/2.4	638/500	2996/870	12060/3120	280/30	103/10
V-22A	1.82/2.06	0.3/2.0	2050/2100	31/1800	49/1700	10/530	29/50
V-22B		1.6/1.6	17405/26000	198/380	275/350	77/80	59/30
V-24	7.07/7.15	1.5/1.6	397/700	1041/1000	1336/1150	158/100	36/30
V-30		2.4/2.8	911/3200	151/880	22754/41000	15/tr	61/30

Slovak Geol. Mag., 8, 1(2002), 21 – 36

24

Ltd., Vancouver, Canada (Table 1). The reproducibility is satisfactory with the exception of zinc because the samples were selected on the base of their gold content and contained little zinc. The difference in gold concentration in the sample V-7 is caused by the presence of metallic gold which cannot be finely ground. It is homogenously distributed in the powdered sample. We have observed metallic gold in this sample in the polished sections.

Oriented mounts of the <2 μm fraction of selected samples of altered rocks were prepared by fine-grinding, ultrasonic disintegration, gravitational sedimentation and coagulation of the fine-grained fraction of the rocks. X-ray diffraction patterns were collected with a Phillips 1710 diffractometer (Geological Institute of Slovak Academy of Science) with CuKα radiation and a Ni filter.

Electron microprobe analyses (EPMA) were performed on JEOL 733 Superprobe (Dionýz Štúr Geological Institute) with these conditions and standards: Pb-Sb sulfosalts: 20 kV, 15 nA, PbS (Pb), FeAsS (Fe, S), metallic Se, Ag, Sb, Bi, Cu, Fe; carbonates: 15 kV, 10 nA, wollastonite (Ca), hematite (Fe), MgO (Mg), rhodonite (Mn); pyrite and arsenopyrite: 20 kV, 20 nA, FeAsS (Fe, As, S), metallic Se, Ag, Sb, Cu, Au, Co, Ni. If possible, several electron microprobe analyses were averaged and the average is reported in tables along with two standard deviations of the mean.

Results

Similarly as most other ore deposits in the Nízke Tatry Mts, the Dve Vody deposit encompasses several types of ore mineralizations. These are the As-Au, Sb, base-metals, and siderite mineralizations, named according to the principal exploited metals or minerals, in agreement with the classification of the ore mineralizations in the Nízke Tatry Mts (Chovan et al. 1996). The samples of the As-Au and Sb mineralizations studied in this work came from the waste dumps of adits 1, 2, 4, and 6 (Fig. 3). The dumps and adits no. 3 and 5, also known to intersect the As-Au and Sb veins (Michálek, 1999), were not identified in the field. The samples of the base-metals mineralization were collected at the dumps of the adits Nová Vyšná and Vyšná Spodná, and the siderite mineralization was sampled from the heaps of four nameless adits in a ravine near elevation point Ždiar (Fig. 1). The three mineralizations occupy separate vein systems (Fig. 1). In the following text, the description of the ore minerals in divided into three parts, according to the distinguished mineralizations. The As-Au and Sb mineralizations are described together because of their close spatial relationship. The information on the distribution of heavy minerals in alluvial sediments and heap material and the chemical composition of the ore samples complements the mineralogical description.

Panning

Heavy mineral concentrates from the alluvial sediments frequently contained minerals that indicated the presence of ore mineralizations in the studied area. Gold flakes were found in most samples of the alluvial sediments (Fig. 3). In the Štellerova dolina valley, gold (2-7 flakes) was found `in every concentrate. Gold was also found in the end of the Kulichova dolina valley. The waste dumps of the adit 2 are rich in gold (up to 220 gold flakes per concentrate). Gold from the dumps has high finesness (Table 2). Most of the gold flakes are smaller than 0.2 mm, similarly as elsewhere in the Nízke Tatry Mts (Fig. 4). Alluvial sediments in the Štellerova dolina valley contain sporadic scheelite (up to 4 grains per concentrate), cassiterite (22), wolframite (1), and cinnabar (2). Common minerals of the concentrates are apatite, zircon, rutile, epidote, pyrite, and limonite. A group of rarer minerals comprises garnet, ilmenite, hematite, monazite, xenotime, and tourmaline.
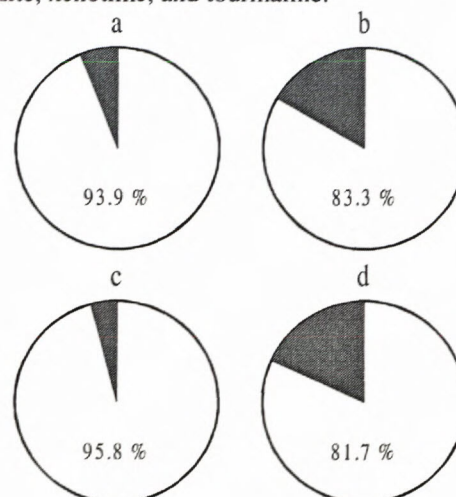

Fig. 4. Proportion of gold grains >0.2 mm (black) and <0.2 mm (gray) in a) alluvial sediments and sandy material of ore waste dumps from Dve Vody (445 gold grains), b) alluvial sediments in Mlynná dolina valley (84) (Majzlan, 1996), c) alluvial sediments in Magurka (3204) (Chovan et al. 1993), d) ore waste dumps from Magurka (465) (Chovan et al. 1993).

Mineral composition of the ore samples

As-Au and Sb mineralization

Arsenopyrite is one of the major minerals of the As-Au mineralization but rarely more abundant than pyrite. Arsenopyrite is found in fine-grained pyrite-arsenopyrite ores hosted by quartz or as impregnations of altered wall-rocks. It forms minute crystals in quartz, often skeletal with core filled by quartz, or inclusions in crystals and fine-grained aggregates of pyrite. Fine-grained arsenopyrite is rarely chemically zonal, as seen in back-scattered electron images (BSEI), and optically zonal with hourglass structure. Coarse-grained arsenopyrite crystals with minor pyrite were occasionally found in altered rock samples (Fig. 5a). Coarse-grained arsenopyrite often displays hourglass structure.

Beside the major elements, arsenopyrite contains only elevated concentrations of Sb (Table 3). Neither cobalt nor copper were detected by electron microprobe analyses

Table 2. Chemical composition (EPMA) of gold from the waste dumps (n.a. = not analyzed).

	Au	Bi	Hg	Cu	Pb	Ag	Te	Sb	total
DV1/1	93.65	0.80	1.15	0.18	0.21	3.66	0.10	n.a.	99.75
DV1/2	94.95	0.72	1.34	0.17	n.a.	3.61	0.19	0.11	101.09
DV2/1	96.86	n.a.	0.73	0.07	0.03	1.18	0.10	n.a.	98.97
DV2/2	97.37	0.16	0.18	0.07	n.a.	1.43	0.08	0.02	99.31
DV3 wt%	92.81	0.53	0.74	0.08	n.a.	5.94	n.a.	0.11	100.21
DV4/1	93.21	0.71	0.57	0.14	0.12	5.43	0.17	0.07	100.42
DV4/2	93.85	0.71	0.33	0.02	n.a.	5.40	0.17	0.11	100.59
DV1/1	90.81	0.73	1.09	0.54	0.19	6.48	0.15	n.a.	
DV1/2	90.83	0.65	1.26	0.50	n.a.	6.31	0.28	0.17	
DV2/1	96.73	n.a.	0.72	0.22	0.03	2.15	0.15	n.a.	
DV2/2	96.71	0.15	0.18	0.22	n.a.	2.59	0.12	0.03	
DV3 at%	88.13	0.47	0.69	0.24	n.a.	10.30	n.a.	0.17	
DV4/1	88.54	0.64	0.53	0.41	0.11	9.42	0.25	0.11	
DV4/2	89.21	0.64	0.31	0.06	n.a.	9.37	0.25	0.17	

Table 3. Chemical composition of arsenopyrite (EPMA) from As-Au mineralization.

	V-10	V-18	V-19
average of	2	6	5
S	21.87 (0.42)	21.40 (0.61)	21.60 (0.66)
Fe	34.96 (0.40)	35.12 (0.17)	35.12 (0.32)
As	40.77 (3.32)	43.12 (1.02)	42.72 (1.00)
Sb wt%	1.88 (3.35)	0.31 (0.20)	0.10 (0.17)
Au	0.17 (0.34)	0.06 (0.02)	0.01 (0.01)
Ni	0.00 (0.00)	0.01 (0.00)	0.01 (0.01)
Total	99.65	100.02	99.56
S	36.50 (0.06)	35.58 (0.81)	35.95 (0.85)
Fe	33.51 (0.31)	33.54 (0.11)	33.56 (0.15)
As	29.12 (1.77)	30.72 (0.86)	30.43 (0.90)
Sb at%	0.84 (1.49)	0.13 (0.08)	0.05 (0.07)
Au	0.05 (0.09)	0.02 (0.01)	0.00 (0.00)
Ni	0.00 (0.00)	0.01 (0.00)	0.01 (0.01)

Table 4.

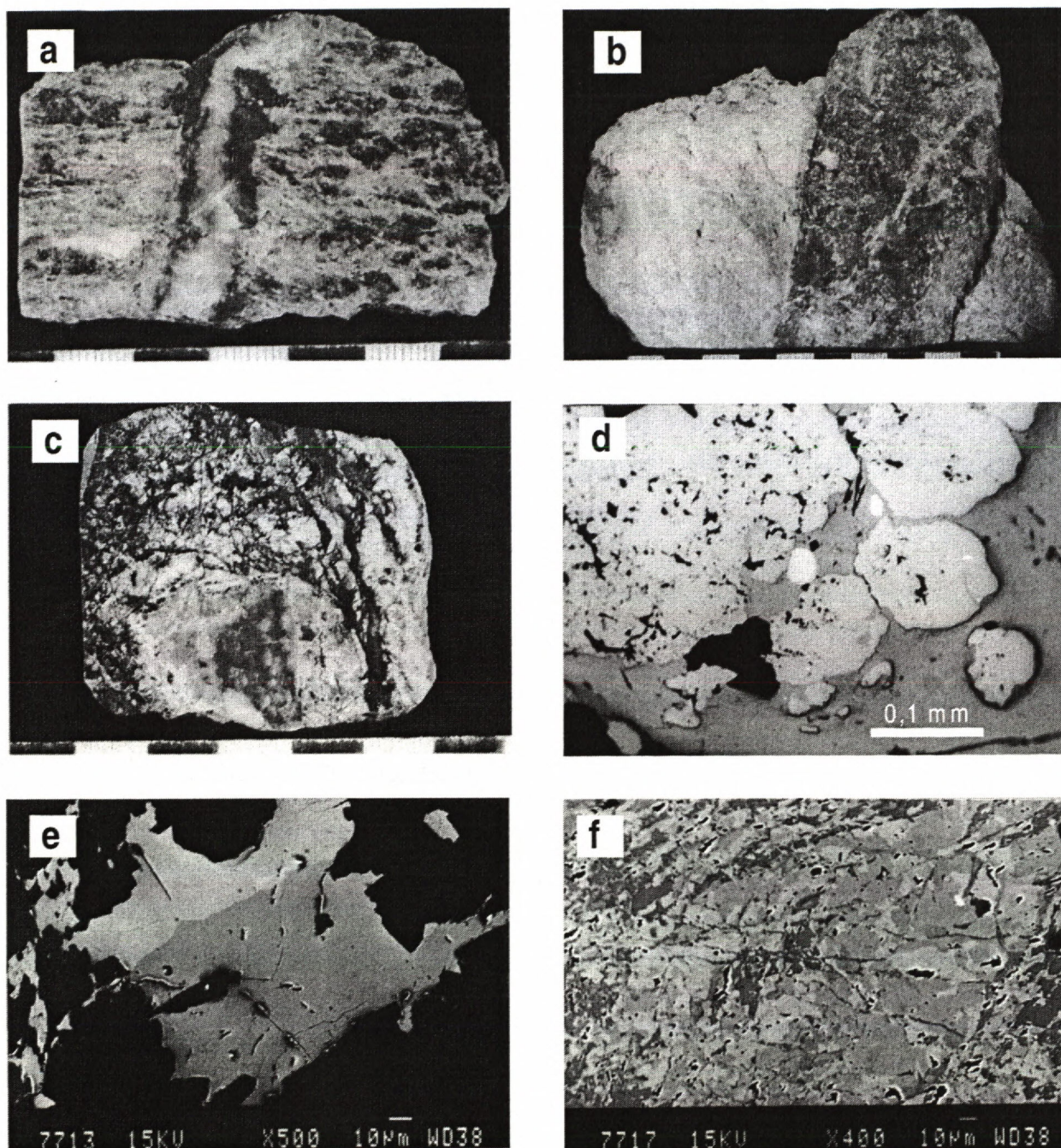|	V-7	V-7	V-7	V-7	V-17A	V-20	V-20	V-20	V-28	V-28	V-43	V-43	V-43	V-43	V-43
Au	95.4	94.26	89.15	90.81	97.44	98.16	96.97	96.94	94.44	94.29	77.01	76.81	66.75	67.84	65.55
Ag	2.92	3.55	3.89	3.71	0.38	0.86	0.66	0.87	0.45	0.17	22.44	22.63	28.05	28.09	30.79
Hg	1.76	0.93	0.99	0.83	0.93	1.33	1.3	1.62	0.55	0.89	0.68	0.8	0.77	0.98	0.92
Cu wt%	0.28	0.24	0.25	0.27	0.29	0.27	0.26	0.29	0.29	0.34	0.22	0.24	0.2	0.2	0.22
Fe	0.08	1.01	0.18	2.95	1.22	0.69	0.67	0.93	-	-	-	-	0.03	0.09	0.09
Total	100.44	99.99	94.46	98.57	100.26	101.31	99.86	100.65	95.88	95.69	100.35	100.48	95.8	97.2	97.57
Au	92.08	88.96	90.38	82.83	93.47	94.11	94.49	92.94	97.66	97.68	64.53	64.19	55.88	56.05	53.00
Ag	5.15	6.12	7.20	6.18	0.67	1.51	1.17	1.52	0.85	0.32	34.34	34.53	42.88	42.38	45.46
Hg at%	1.67	0.86	0.99	0.74	0.88	1.25	1.24	1.53	0.56	0.91	0.56	0.66	0.63	0.80	0.73
Cu	0.84	0.70	0.79	0.76	0.86	0.80	0.79	0.86	0.93	1.09	0.57	0.62	0.52	0.51	0.55
Fe	0.27	3.36	0.64	9.49	4.13	2.33	2.30	3.14	-	-	-	-	0.09	0.26	0.26

Slovak Geol. Mag., 8, 1(2002), 21 – 36

26

Fig. 5. a) altered rock impregnated by coarse-grained gold-bearing arsenopyrite, with a quartz veinlet with arsenopyrite minerali-zation (sample V-18); scale in cm; b) the contact of white quartz (cf. V-22A, Table 12) with no gold and gray quartz (V-22B, Table 12) with fine-grained pyrite and arsenopyrite, rich in gold; scale in cm; c) fragment of quartz with As-Au mineralization (pyrite, arsenopyrite) with a rim of sphalerite enclosed in carbonate-sulphosalt-stibnite matrix (V-26A), scale in cm; d) electrum inclusions (bright) in galena (gray) with pyrite crystals (V-43); (reflected light); e) intergrowths of zinckenite (darker gray) and robinsonite (brighter) in carbonate (black) (cf. EPMA analyses of sample V-26A, Table 5, Fig. 6) (SEM), f) intergrowth of carbonate species in V-26A (cf. Table 10a, Fig. 7a). Brighter gray are siderite I and II, replaced by calcite (darker gray). Quartz is black, sulfosalt inclu-sion is bright (SEM).

(EMPA). Low concentrations of gold and nickel (EMPA) are questionable without confirmation by a more sensitive analytical technique.

Stibnite hosts minute euhedral arsenopyrite crystals that were probably formed during the initial stages of Sb-sulfides precipitation.

Berthierite is encountered rarely, intimately inter-grown with stibnite. Pink tint in parallel nicols and reflec-tivity slightly lower than that of stibnite distinguish berthierite from stibnite in reflected light.

Bournonite is rare, intergrown with Pb-Sb sulfosalts, stibnite, and tetrahedrite. It corrodes and replaces tetra-

hedrite and pyrite. In reflected light, bournonite has gray-ish color, moderately low reflectivity (lower than Pb-Sb sulfosalts), orange and blue anisotropy effect and typical polysynthetic twinning.

Gold is relatively frequent on microscopic scale. No macroscopic gold was observed in hand specimens from the dumps. Gold is associated with fine-grained pyrite and arsenopyrite, occasionally replacing pyrite. Stibnite impregnating fine-grained pyrite and arsenopyrite encloses gold grains. Minute gold grains and dendritic aggregates accompany Pb-Sb sulfosalts. High fineness is characteristic for both gold associated with Fe-As sulfides (90.1 at.% Au) and Sb sulfides (96.2 at.% Au) (Table 4). Small size of some gold grains is responsible for low totals of some microprobe analyses.

Pb-Sb sulfosalts are found commonly, with or without stibnite. The aggregates of Pb-Sb sulfosalts, up to several cm large, are composed of milimetre-sized needle-like crystals. The sulfosalts usually penetrate along grain boundaries of carbonates or forms rims of the quartz veinlets in carbonates. They can also be seen on quartz veinlets that penetrate into the fine-grained pyrite-arsenopyrite ores. We have occasionaly found minute needles of Pb-Sb sulfosalts uniformly dispersed in Fe-dolomite, suggesting their contamporaneous crystallization. The optical properties of Pb-Sb sulfosalts are almost identical for the species encountered in this study. In reflected light, they have white color, inconspicuous birefrigerance, lower reflectivity than stibnite and weaker anisotropy than stibnite. Needles of zinckenite can be distinguished by their parallel extinction, as opposed to oblique extinction of the other sulfosalt species.

EMPA analyses (Table 5) have identified a variety of sulfosalt species. The most common sulfosalt is zinckenite. Robinsonite is intergrown with zinckenite (Fig. 5b) or forms minute needles and grains with inclusions of boulangerite. Heteromorfite is found as small tabular crystals with boulangerite inclusions. The lead to copper ratio in the Pb-Sb sulfosalts is plotted in Fig. 6 versus the copper content. In agreement with crystal-chemical studies of sulfosalts (Moëlo, 1982), the tolerance of Pb-Sb sulfosalts for copper is low, with the exception of Cu-zinckenite. Co-existing zinckenite and robinsonite (Fig. 5b) display significantly different copper content (composition of the co-existing phases is indicated by a tie line in Fig. 6).

Pyrite is one of the most abundant minerals in the deposit. The oldest pyrite generation is represented by fine-grained pyrite aggregates, almost always with some arsenopyrite. Fine-grained pyrite and arsenopyrite impregnate vein quartz or altered wallrocks (Fig. 5c). This type of pyrite is characteristic by hexahedral habitus, chemical homogeneity (BSEI) with generally low arsenic content (Table 6), and crystal size averaging 10-20 μm, rarely exceeding 50 μm. Uncommon chemical zonality is caused by variable arsenic concentration (0 to 2.55 at.% As) (Table 7).

Pyrite is also abundant in stibnite and Pb-Sb sulfosalt ores. In contrast to the older fine-grained pyrite, here it forms larger (up to 1 mm) subhedral to euhedral pentago-

nal dodecahedral crystals. Pyrite crystals are often constituted of a core separated from the rim by a zone of quartz inclusions (photo). These pyrite crystals are homogeneous, with low arsenic content (Table 6). Electron microprobe detected no Se, Co, Sb, and Cu. Most of the measured nickel and gold concentrations are below the EPMA detection limit.
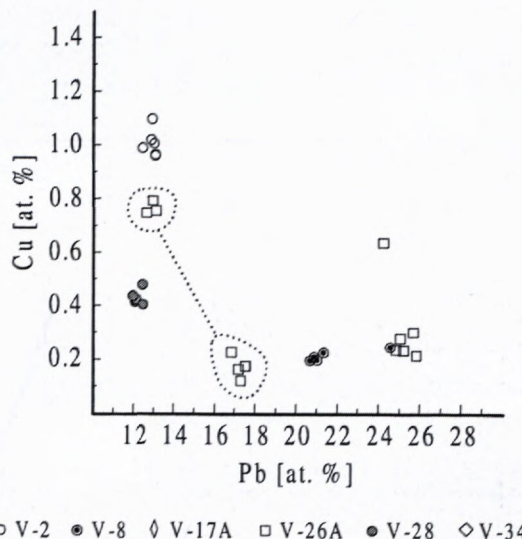

Fig. 6. Chemical composition of the sulfosalts from Dve Vody, in terms of their Pb vs. Cu content. Two marked fields, connected by a line represent the composition of co-existing of robinsonite and zinckenite (see Fig. 5e).

Sphalerite is found with Pb-Sb sulfosalts or separately in the gangue minerals. It forms grains of honey-yellow to brown color, up to 5 mm large. Beside the major elements, electron microprobe detected up to 0.24 at.% Fe, 0.10 at.% Cd, 0.10 at.% Mn, 0.07 at.% Sn and no Hg (Table 8). Sphalerite crystallized earlier than Pb-Sb sulfosalts (Fig. 5d).

Stibnite is the principal mineral of the Sb mineralization, forming aggregates of cm size in white quartz. It also forms monomineral veinlets in altered rocks, preferentially developed in porfyroblasts of the rock-forming quartz, only rarely emplaced in muscovite along the cleavage planes. Stibnite penetrates into the older fine-grained pyrite and arsenopyrite. There are infrequent stibnite relics in aggregates of Pb-Sb sulfosalts. The characteristic mosaic aggregates of stibnite carry few signs of tectonic deformation such undulose extinction or pressure-induced recrystallization.

Tetrahedrite is a scarce mineral in the Sb mineralization, intimately intergrown with bournonite.

Carbonates are common but not as abundant as quartz. The color of the polycrystalline carbonate aggregates varies from white to deep brown. Veinlets of fine-grained carbonates croscutting older, coarser carbonates witness episodic remobilization and tectonization of the mineralization. Later stages of carbonate remobilization were accompanied by minor amount of quartz and Pb-Sb sulfosalts.

Slovak Geol. Mag., 8, 1(2002), 21 – 36

28

Table 5. Chemical composition (EPMA) of sulfosalts from Sb (V-2, V-26A, V-28, V-8) and base-metals (V-34) mineralization.

	Pb	Sb	Cu	Fe	S	Se	Total	Pb	Sb	Cu	Fe	S	Se
				wt%						at%			
V-28	31.39	45.58	0.33	0.04	22.89	0.01	100.24	12.16	30.05	0.42	0.06	57.30	0.01
V-28	32.21	44.78	0.38	0.05	22.81	0.00	100.23	12.52	29.62	0.48	0.07	57.30	0.00
V-2	32.00	43.99	0.78	0.06	22.50	0.11	99.44	12.53	29.32	1.00	0.09	56.95	0.11
V-2	32.92	42.09	0.78	0.07	22.24	0.00	98.10	13.11	28.53	1.01	0.10	57.24	0.00
V-2	32.94	42.87	0.80	0.04	22.46	0.07	99.18	12.97	28.72	1.03	0.06	57.14	0.08
V-2	33.18	43.18	0.75	0.03	22.00	0.08	99.22	13.19	29.21	0.97	0.04	56.50	0.08
V-26A	32.58	43.77	0.59	0.27	22.51	0.05	99.77	12.75	29.14	0.75	0.39	56.91	0.05
V-26A	33.60	43.97	0.63	0.06	22.72	0.00	100.98	13.05	29.06	0.80	0.09	57.01	0.00
V-26A	33.95	43.74	0.60	0.05	22.65	0.02	101.01	13.21	28.97	0.76	0.07	56.96	0.02
V-26A	41.18	36.78	0.17	0.27	21.15	0.12	99.67	16.99	25.83	0.23	0.41	56.40	0.13
V-26A	41.46	36.45	0.12	0.07	20.80	0.08	98.98	17.37	25.98	0.16	0.11	56.30	0.08
V-26A	42.23	36.82	0.09	0.28	21.00	0.00	100.42	17.46	25.90	0.12	0.43	56.09	0.00
V-26A	42.40	35.85	0.13	0.21	20.88	0.00	99.47	17.70	25.47	0.18	0.33	56.33	0.00
V-8	48.57	31.09	0.14	0.06	19.59	0.00	99.45	21.23	23.13	0.20	0.10	55.34	0.00
V-8	48.74	31.00	0.15	0.07	19.95	0.00	99.91	21.09	22.82	0.21	0.11	55.77	0.00
V-8	55.52	25.82	0.17	0.09	19.05	0.00	100.65	24.85	19.66	0.25	0.15	55.09	0.00
V-34	54.95	25.22	0.16	0.08	18.52	0.00	98.93	25.16	19.66	0.24	0.14	54.81	0.00
V-34	55.84	25.45	0.19	0.05	18.60	0.00	100.13	25.37	19.67	0.28	0.08	54.60	0.00
V-34	56.17	25.10	0.16	0.07	18.64	0.00	100.14	25.52	19.41	0.24	0.12	54.72	0.00
V-34	86.42	0.00	0.20	0.10	13.49	0.05	100.26	49.46	0.00	0.37	0.21	49.89	0.07

Table 6. Chemical composition of pyrite (EPMA) from As-Au (V-6, V-7, V-10), Sb (V-31), and base-metals (V-36) mineralization.

	V-6	V-7	V-10	V-19	V-31	V-36
average of	4	3	2	1	4	3
S	54.67 (0.97)	54.07 (0.16)	55.04 (0.60)	55.35	53.66 (1.98)	54.07 (0.37)
Fe	44.90 (0.51)	44.95 (0.23)	45.04 (0.99)	46.11	45.30 (0.50)	44.95 (0.50)
As	0.00 (0.00)	1.74 (0.68)	0.17 (0.09)	0.28	0.73 (1.46)	0.06 (0.13)
Sb	n.a.	n.a.	n.a.	n.a.	n.a.	n.a.
Au	0.12 (0.12)	0.08 (0.17)	0.03 (0.05)	0.00	0.04 (0.05)	0.00 (0.00)
Ni	0.00 (0.01)	0.00 (0.00)	0.03 (0.02)	0.00	0.01 (0.01)	0.01 (0.02)
Total	99.69	100.85	100.29	101.74	99.75	99.10
S	67.94 (0.42)	67.06 (0.23)	67.96 (0.68)	67.55	67.07 (1.16)	67.67 (0.14)
Fe	32.04 (0.43)	32.00 (0.18)	31.93 (0.73)	32.30	32.52 (0.37)	32.29 (0.14)
As	0.00 (0.00)	0.92 (0.36)	0.09 (0.04)	0.14	0.40 (0.81)	0.03 (0.07)
Sb	n.a.	n.a.	n.a.	n.a.	n.a.	n.a.
Au	0.03 (0.02)	0.02 (0.03)	0.01 (0.01)	0.00	0.01 (0.01)	0.00 (0.00)
Ni	0.00 (0.01)	0.00 (0.00)	0.02 (0.01)	0.00	0.01 (0.01)	0.01 (0.01)

Table 7. Chemical composition (EPMA) of zonal pyrite (sample V-15, Sb mineralization) arranged from the darkest (as seen in BSEI) to the lightest zone from left to right.

	darkest					lightest
S	55.17	54.97	55.11	53.29	51.45	51.55
Fe	45.52	45.80	46.16	45.68	44.18	45.30
As wt%	0.00	0.00	0.00	1.51	4.69	4.20
Au	0.00	0.15	0.00	0.00	0.01	0.10
Ni	0.00	0.03	0.00	0.00	0.00	0.00
Total	100.69	100.94	101.27	100.49	100.32	101.15
S	67.86	67.61	67.53	66.48	65.27	64.95
Fe	32.14	32.34	32.47	32.71	32.18	32.77
As w t%	0.00	0.00	0.00	0.81	2.55	2.27
Au	0.00	0.03	0.00	0.00	0.00	0.02
Ni	0.00	0.02	0.00	0.00	0.00	0.00

Manometric analyses (Table 9) distinguished siderite and ankerite. A more detailed study with electron microprobe showed presence of two Fe-rich carbonates, siderite I and siderite II (Table 10a, Fig. 5e). Siderite appears to be the earliest carbonate in the deposit. Deposition of siderite is followed by precipitation of Fe-dolomite or calcite (Table 10b). Calcite encloses rare inclusions of magnesite. The magnesite inclusions were too small to obtain a reliable EPMA analysis, but an approximate composition can be read from Fig. 7a. Compositional differences and paragenetic relationships between these carbonates were observable only in back-scattered electron images.
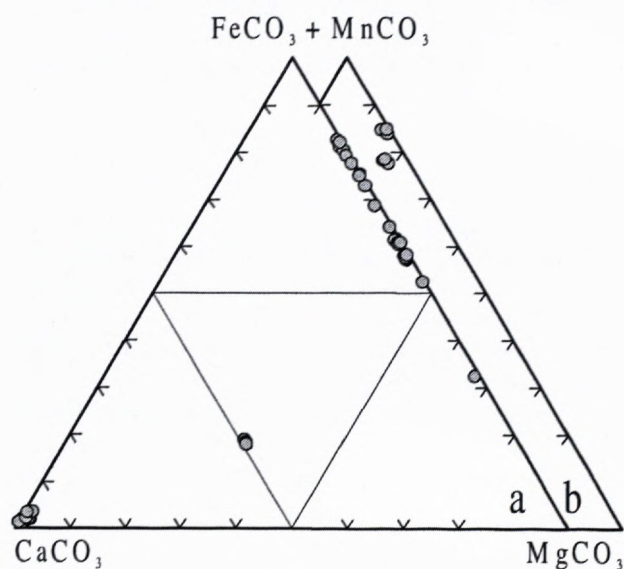

Fig. 7. Chemical composition of carbonates from Dve Vody. a) Sb mineralization, b) siderite mineralization.

A fine-grained mineral ubiquitos in the altered wall-rocks has been identified by X-ray diffraction analyses as **illite**. The mica-like aggregates partially or completely replace porphyroblasts of feldspars. Strongly altered rocks are composed only of quartz and illite with impregnations of sulfides. Less intensively altered rocks contain also large flakes of **muscovite**. It is not clear whether muscovite was formed during hydrothermal alteration of the wall-rocks or was an original component of the metamorphic rocks. Minute mica-like crystals were commonly found in vein quartz with Pb-Sb sulfosalts.

Quartz is the most abundant mineral of the ore veins. It accompanies almost all sulfidic minerals, with the exceptions of the monomineral stibnite veinlets. Grayish color of some quartz specimens is caused by impregnations of sulfides, predominantly fine-grained pyrite and arsenopyrite. Grayish quartz, with the associated sulfides, is the principal gold carrier in the deposit. According to our petrographic observations and chemical analyses, white quartz with no sulfide minerals contains virtually no gold.

Minute grains of Ti-minerals are frequent in strongly altered wall-rocks. Optical properties of these grains correspond to the optical properties of **rutile** and **ilmenite**.

Base-metals mineralization

Two oval inclusions of **electrum** were found in an aggregate of galena and pyrite (Fig. 5f). Electrum contains 58.7 at.% Au (Table 4).

Galena is one of the major sulfidic mineral of the mineralization. It forms large (up to several cm) aggregates, accompanied by abundant pyrite and quartz. Concentration of silver as determined by EPMA is low (Table 5).

Pb-Sb sulfosalts are a common component of the base-metals mineralization. Needle-like crystals and crystalline aggregates of the sulfosalts are locally more abundant than galena. Galena often encloses small inclusions of sulfosalts. The sulfosalts were identified by electron microprobe analyses (Table 5, Fig. 6) as boulangerite.

Pyrite and galena are the principal ore minerals. Subhedral, rarely euhedral pyrite crystals are often replaced by galena, sphalerite, and Pb-Sb sulfosalts. Massive monomineralic pyrite aggregates are common. Pyrite crystals are frequently composed of a core separated from the rim by a number of minute quartz inclusions. Some of the pyrite crystals display unusually strong anomalous anisotropy.

Sphalerite is common, invariably earlier than the sulfosalts. Beside the major elements, it contains only traces of Mn and Sn (Table 8).

Tetrahedrite is found seldomly as small oval inclusions in galena. According to the EPMA analyses (Table 11), tetrahedrite is the only silver-bearing mineral of the base-metals mineralization.

Carbonates are infrequent, often replaced by earthy mass of hydrated iron oxides.

Quartz is abundant, massive, usually grayish in color owing to the sulfide inclusions.

Siderite mineralization

Bournonite is one of the dominating sulfidic minerals of the siderite mineralization. Bournonite or intergrowths of bournonite and tetrahedrite form grains up to several cm large.

Small anhedral grains of **chalcopyrite** are infrequently found with other Cu sulfides, galena, and pyrite.

Isolated minute grains (< 0.5 mm) or veinlets of **galena** in quartz are rare. Galena is also found as inclusions in bournonite or along the contact of bournonite and tetrahedrite grains.

Massive aggregates of **tetrahedrite** in quartz or intergrowths of tetrahedrite and bournonite are common. According to the EPMA analyses (Table 11), the Ag content of tetrahedrite is low (< 1 wt.%), the tetrahedral M1 site is occupied dominantly by zinc, and the tennantite component fraction is low (< 6 mol.%).

Siderite forms mostly fine-grained massive aggregates, commonly cross-cut by veinlets of coarser carbonate. Electron microprobe (Fig. 7b, Table 10b) and manometric analyses (Table 9) identified only carbonate compositions classifiable as siderite.

Quartz is significantly less abundant than siderite, white in color, forming grains in siderite.

Table 8. Chemical composition (EPMA) of sphalerite from Sb (V-25, V-26A) and base-metals (V-41) mineralization.

Sample		V-25	V-26A	V-41
average of		4	4	4
S		32.65(0.40)	32.67(0.38)	32.78(0.37)
Zn		66.82(0.55)	67.05(0.24)	67.52(0.27)
Cu		-	-	-
Fe	wt%	0.24(0.02)	0.17(0.09)	-
Cd		0.18(0.07)	0.17(0.04)	-
Sn		0.15(0.03)	0.14(0.02)	0.13(0.02)
Hg		-	-	-
Mn		0.05(0.02)	0.04(0.04)	0.08(0.05)
Total		100.06(0.68)	100.16(0.20)	100.47(0.67)
S		49.72(0.37)	49.71(0.36)	49.71(0.19)
Zn		49.91(0.37)	50.04(0.40)	50.21(0.20)
Cu		-	-	-
Fe	at%	0.21(0.02)	0.15(0.08)	-
Cd		0.07(0.03)	0.08(0.02)	-
Sn		0.06(0.01)	0.06(0.01)	0.05(0.01)
Hg		-	-	-
Mn		0.05(0.01)	0.04(0.04)	0.07(0.04)

Table 9. Chemical composition (manometric analyses) of carbonates from Sb (V-8, V-17A, V-23D) and siderite (V-48) mineralization.

	S^a	D^b	IR^c	CaO	MgO	FeO
V-8	79.24	3.26	24.30	0.99	11.63	30.76
V-17A	-	92.33	0.76	29.28	17.33	6.66
V-23D	-	91.29	2.65	28.61	16.37	7.47
V-48	96.41	-	7.63	-	6.60	48.71

[a] per cent of the siderite component
[b] per cent of the dolomite component
[c] per cent of insoluble residuum

Chemical composition of the ore samples

The results of chemical analyses of the ore sample from the Dve Vody deposit can be correlated with the mineral composition as determined by optical microscopy (Table 12). The relationships between elemental concentrations in the analyzed samples are shown in Fig. 8. A corelation matrix of the metal concentrations is shown in Table 13.

Elevated gold concentrations were recorded in samples of the fine-grained pyrite-arsenopyrite ores (V-18, V-19, V-22B), more rarely in samples with Pb-Sb sulfosalts (samples V-20, V-28) and stibnite (V-30). Fig. 5c shows a typical example of white quartz with no sulfidic mineralization that contains little gold and gray quartz impregnated with pyrite and arsenopyrite rich in gold (cf. Au analyses for V-22A (white quartz) and V-22B (gray quartz), Table 12). This relationship documents the importance of fine-grained pyrite-arsenopyrite as the gold ore. Furthermore, no metallic gold was found in several arsenopyrite-rich samples with elevated gold content (V-18, V-19), suggesting that gold in these samples is chemi-

cally bound in arsenopyrite. On the other hand, a significant portion of gold occurs as metallic gold. The highest gold concentration was recorded in samples with low Sb content (Fig. 8a), stressing a relatively insignificant role of the Sb sulfides as gold carriers. We found gold grains enclosed in stibnite, however, they seem to have existed, together with pyrite and arsenopyrite, before the stibnite was emplaced. A comparison of gold and arsenic content (Table 12) in bulk samples suggests that arsenopyrite should contain 200-300 ppm Au (Fig. 8b), assuming that arsenopyrite is the only arsenic- and gold-bearing phase in those samples. The assumption may be incorrect where pyrite is present in larger amounts as it can contain both As and Au. Despite the neglect of pyrite presence in our samples, the estimated gold concentration of 200-300 ppm (Fig. 8b) compares well to the range of gold content in arsenopyrite from other deposits (Cabri, 1992). Arsenopyrite crystals from the sample V-18 were analyzed for gold by atomic absorption spectroscopy. The crystals were briefly leached, and the leachate was believed to represent the chemical composition of the outer portion of the crystals, giving 170 ppm of Au for this part of the crystals. A complete dissolution and correction for the outer portion gave a concentration of 99 ppm for the inner portion of the arsenopyrite crystals.

Lead and antimony are found either separately in galena (samples V-36, V-45) and stibnite (V-10, V-29, V-30) or combined in Pb-Sb sulfosalts (V-25, V-26, V-26A), as indicated by Fig. 8c. The principal carrier of Pb and Sb in the samples V-49 and V-50 is bournonite.

The observation of common occurrence of sphalerite and Pb-Sb sulfosalts is corroborated also by the chemical relationship between Pb and Zn (Fig. 8d). The association of sphalerite and Pb-Sb sulfosalts was observed both in the Sb and base-metals mineralization.

As-Au, Sb and base-metals mineralizations have only insignificant copper content. The dominant role of bournonite in the siderite mineralization (samples V-49 and V-50) is conspicuous from elevated concentration of Pb and Cu in these samples (Fig. 8e).

Higher silver content was observed in some samples of the Sb mineralization (V-25, V-26, and V-26A), correlating with their Pb content (Fig. 8f, Table 13). The mineral composition of these samples (pyrite, arsenopyrite, sphalerite, stibnite, Pb-Sb sulfosalts) indicates that most silver should be found in the sulfosalts. Calculation from bulk-rock analyses (Table 12) shows that the sulfosalts should contain 200-800 ppm of silver to account fully for all silver in the samples. However, electron microprobe analyses record no silver in the sulfosalts. Another possibility is accumulation of silver in submicroscopic Ag phases or Ag-rich domains in the sulfosalts. Abundance of galena and high silver content in the samples of the base-metals mineralization hint that silver is found dominantly in this mineral but microprobe analyses show no silver in galena. According to EPMA, the only mineral of the base-metals mineralization with significant Ag content is scarce tetrahedrite. The principal carrier of silver in the siderite mineralization (V-49, V-50) is tetrahedrite.

Table 10a. Chemical composition (EPMA) of carbonates from Sb mineralization.

	V-8	V-8	V-8	V-8	V-26A. sid I	V-26A. cc	V-26A. sid II	V-26A. mez
average of	1	2	2	3	4	4	2	1
FeO	45.06	40.73 (0.12)	36.85 (1.36)	0.54 (0.46)	48.73 (1.10)	1.69 (0.43)	40.09 (2.24)	24.02
MgO	11.61	14.17 (1.36)	17.26 (1.92)	0.18 (0.21)	8.71 (1.24)	0.39 (0.17)	15.49 (1.54)	28.88
CaO wt%	0.48	0.35 (0.11)	0.45 (0.22)	54.77 (0.60)	0.30 (0.07)	53.30 (0.88)	0.54 (0.05)	0.61
MnO	1.32	2.37 (0.37)	2.61 (0.23)	0.59 (0.14)	1.83 (0.05)	0.61 (0.32)	1.23 (0.27)	1.00
SrO	0.00	0.00 (0.00)	0.00 (0.00)	0.88 (0.29)	0.00 (0.00)	0.00 (0.00)	0.00 (0.00)	0.00
Total	58.47	57.61	57.16	56.96	59.56	55.99	57.34	54.51
$FeCO_3$	72.66	65.68 (0.20)	59.42 (2.20)	0.87 (0.74)	78.58 (1.77)	2.73 (0.70)	64.65 (3.61)	38.73
$MgCO_3$	24.29	29.65 (2.85)	36.10 (4.01)	0.37 (0.43)	18.21 (2.61)	0.81 (0.34)	32.40 (3.22)	60.42
$CaCO_3$ wt%	0.86	0.62 (0.19)	0.80 (0.39)	97.75 (1.08)	0.53 (0.12)	95.14 (1.57)	0.96 (0.09)	1.09
$MnCO_3$	2.14	3.83 (0.60)	4.22 (0.36)	0.96 (0.23)	2.97 (0.08)	0.99 (0.53)	1.99 (0.43)	1.62
$SrCO_3$	0.00	0.00 (0.00)	0.00 (0.00)	1.25 (0.42)	0.00 (0.00)	0.00 (0.00)	0.00 (0.00)	0.00
Total	99.95	99.77	100.54	101.20	100.29	99.66	99.99	101.86

Table 10b. Chemical composition (EPMA) of carbonates from Sb (V-2, V-6, V-17A, V-23D) and siderite (V-47) mineralization.

	V-2	V-6	V-17A. ank	V-17A. sid	V-23D	V-47
average of	4	5	3	4	2	6
FeO	0.84 (0.05)	49.43 (1.61)	12.94 (0.33)	41.00 (0.99)	9.59 (0.09)	50.93 (1.38)
MgO	0.61 (0.07)	6.96 (1.06)	13.26 (0.20)	15.49 (0.50)	14.04 (0.13)	5.96 (0.60)
CaO wt%	54.10 (1.05)	0.29 (0.11)	27.80 (0.09)	0.31 (0.14)	27.10 (0.02)	1.31 (0.74)
MnO	0.63 (0.05)	2.32 (0.28)	0.36 (0.03)	0.88 (0.11)	0.78 (0.21)	2.14 (0.33)
SrO	0.00 (0.00)	0.00 (0.00)	0.00 (0.00)	0.00 (0.00)	0.00 (0.00)	0.00 (0.00)
Total	56.18	59.00	54.37	57.67	51.50	60.34
$FeCO_3$	1.35 (0.07)	79.71 (2.60)	20.87 (0.52)	66.11 (1.59)	15.46 (0.15)	82.13 (2.23)
$MgCO_3$	1.28 (0.14)	14.55 (2.21)	27.74 (0.41)	32.40 (1.03)	29.36 (0.28)	12.47 (1.26)
$CaCO_3$ wt%	96.56 (1.87)	0.52 (0.20)	49.62 (0.16)	0.55 (0.26)	48.37 (0.03)	2.34 (1.32)
$MnCO_3$	1.02 (0.09)	3.76 (0.46)	0.59 (0.05)	1.43 (0.18)	1.26 (0.34)	3.47 (0.53)
$SrCO_3$	0.00 (0.00)	0.00 (0.00)	0.00 (0.00)	0.00 (0.00)	0.00 (0.00)	0.00 (0.00)
Total	100.21	98.55	98.82	100.48	94.44	100.40

Table 11. Chemical composition (EPMA) of tetrahedrite (Se. Hg. Bi not detected) from Sb (V-17), base-metals (V-43), and siderite (V-49) mineralization.

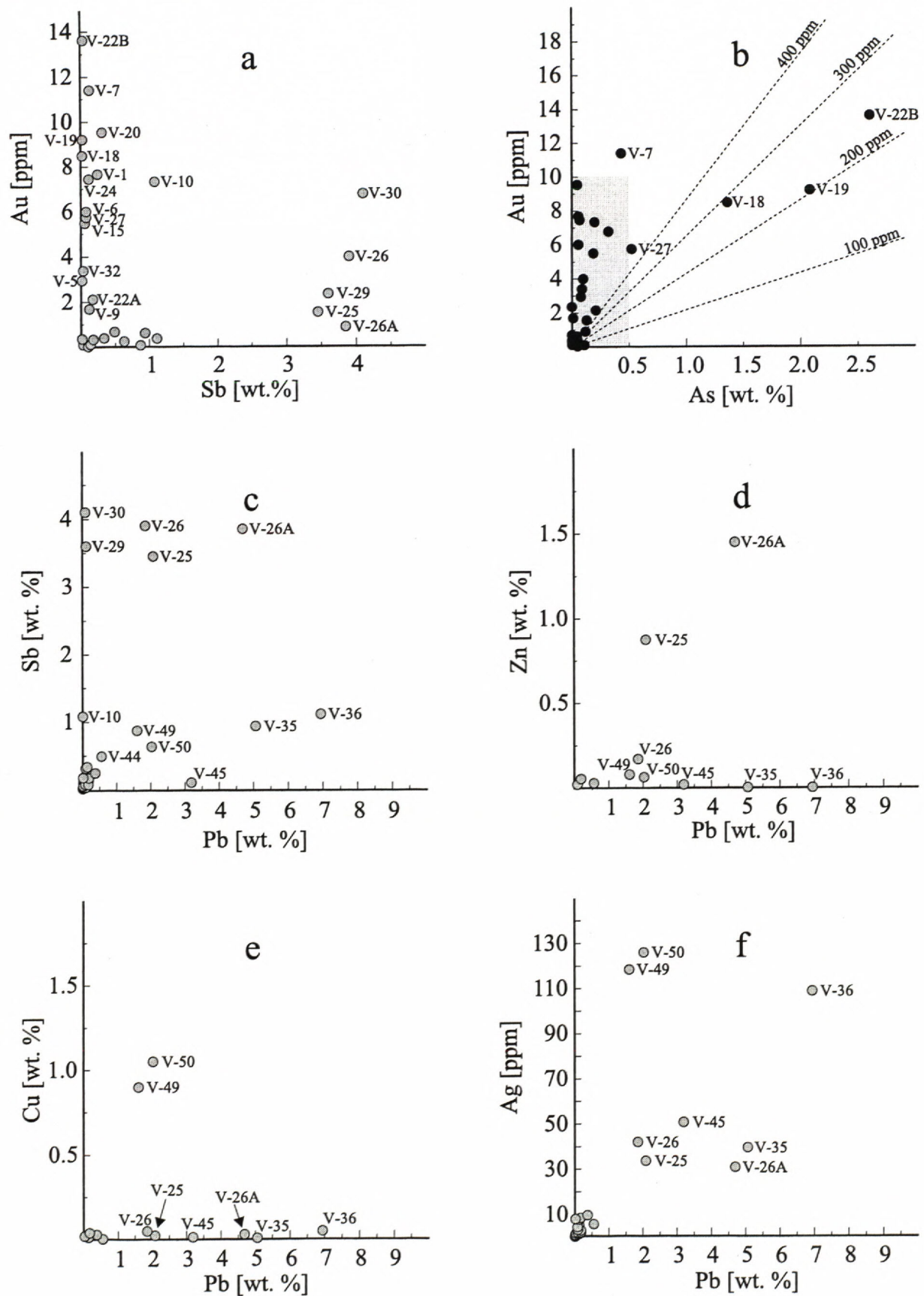| Sample	V-49	V-49	V-49	V-49	V-49	V-49	V-48	V-43	V-17	V-17	V-17
Cu	37.34	37.51	37.58	37.6	37.38	37.61	37.57	36.18	34.42	34.43	34.26
Ag	0.84	0.57	0.98	0.55	0.97	0.86	0.92	2.44	5.02	5.3	4.85
Zn	6.34	6.54	6.38	6.21	6.33	6.34	4.97	6.32	1.48	1.55	2.01
Fe wt%	1.04	0.98	0.95	0.93	1.01	0.98	2.05	1.06	4.83	4.6	4.34
Sb	28.6	28.56	28.63	28.96	28.07	28.48	26.99	28.37	25.88	25.81	26.06
As	0.27	0.4	0.15	0.27	0.25	0.37	0.92	0.64	0.82	0.84	1.1
S	23.61	23.77	24.01	24.22	24.21	24.01	24.74	23.51	23.8	23.93	23.88
Total	98.03	98.31	98.68	98.72	98.22	98.65	98.15	98.51	96.25	96.44	96.51
Cu	34.86	34.84	34.77	34.70	34.58	34.77	34.41	33.84	32.57	32.51	32.36
Ag	0.46	0.31	0.53	0.30	0.53	0.47	0.50	1.34	2.80	2.95	2.70
Zn	5.75	5.90	5.74	5.57	5.69	5.70	4.42	5.74	1.36	1.42	1.85
Fe at%	1.10	1.04	1.00	0.98	1.06	1.03	2.14	1.13	5.20	4.94	4.66
Sb	13.93	13.84	13.82	13.95	13.55	13.74	12.90	13.85	12.78	12.72	12.85
As	0.21	0.32	0.12	0.21	0.20	0.29	0.71	0.51	0.66	0.67	0.88
S	43.68	43.75	44.02	44.30	44.39	44.00	44.91	43.58	44.63	44.78	44.70

Fig. 8. Graphical representation of the chemical composition of ore samples from Dve Vody.

mineralizations	hydrothermal alteration	As-Au	Sb			base-metals	siderite
parageneses			carbonate	sphalerite-sulfosalt	stibnite		
illite	—						
muscovite	—						
Ti-oxides							
quartz		—		—		—	
arsenopyrite		—					
pyrite		—		—		—	
gold		—					
Fe-dolomite			—				
sphalerite				—			
zinckenite				—			
stibnite					—		
berthierite					—		
galena						—	
siderite			—				—
tetrahedrite							—
bournonite							—
chalcopyrite							—

Fig. 9. Paragenetic sequence of the Dve Vody deposit.

Discussion and conclusions

The mineralizations distinguished in the Dve Vody deposit correspond, in terms of their mineralogical and chemical composition, to the mineralizations elsewhere in Nízke Tatry Mts as classified by Chovan et al. (1996). These are the As-Au, Sb, base-metals, and siderite mineralizations, listed in the order in which they were formed. The paragenetic sequence for the deposit, based on the observations made in this study and previous work (Kantor, 1948, Hak, 1966) is shown in Fig. 9. Penetration of quartz veinlets with Sb sulfides into brecciated As-Au mineralization documents the temporal relationship between the As-Au and Sb mineralization. An intersection of a stibnite vein (Sb mineralization) by a galena vein (base-metals mineralization) in Nová Vyšná adit (Kantor & Rybár, 1964) proves later deposition of the base-metals mineralization. According to Michálek (1999), the ores of As-Au, Sb, and base-metals mineralization occupy tectonic structures opened during the first deformation stage. The latest siderite mineralization fills structures created during the second deformation stage (Michálek, 1999).

The early As-Au mineralization, represented by fine-grained pyrite-arsenopyrite ores, is a typical feature of many ore deposits in the Nízke Tatry Mts. At the Dve Vody deposit, these ores are the most important gold carrier, either in chemical form in arsenopyrite and pyrite or as metallic gold. In contrast with the deposit Magurka (Chovan et al. 1995), the gold concentration at Dve Vody is low in white quartz devoid of sulfides, as opposed to

high gold content of gray quartz impregnated by fine-grained Fe-As sulfides (Fig. 5c). The abundance of metallic gold in the fine-grained pyrite-arsenopyrite ores is exceptional compared to other ore deposits in the Nízke Tatry Mts.

Rare brecciated textures (Fig. 5d), consisting of fragments of As-Au mineralization enclosed by the Sb mineralization document the temporal relationship among the two mineralizations. The Sb mineralization can be divided into three parageneses. The first one is rich in carbonates that are surprisingly variable in their chemical composition (Fig. 5e), especially in comparison with other deposits in the Nízke Tatry Mts. The second paragenesis comprises sphalerite and sulfosalts, usually associated with carbonates. On the other hand, stibnite, the most abundant sulfide of the third paragenesis, is found mostly in quartz or in monomineralic veins in altered rocks. The paragenetic sequence of the three parageneses within the Sb mineralization is not completely clear. There is satisfactory textural evidence that the major portion of the carbonates is earlier than sphalerite and sulfosalts, sphalerite being always earlier than sulfosalts. On the other hand, little information was gathered about the relationship between sulfosalts and stibnite. Rare irregular relics of stibnite in sulfosalts or zinckenite veinlets cutting through stibnite aggregates suggest that the sulfosalts were emplaced after the deposition of stibnite. Similar observations were recently documented from ore samples from Klačianka (Bakos et al. 2000). These infrequent occurrences are, in our opinion, an insufficient proof of

34

Slovak Geol. Mag., 8, 1(2002), 21 – 36

*Table 12. Chemical and mineralogical composition of the samples from Dve Vody. Mineral abbreviations: asp – arsenopyrite, py – pyrite, Au – gold, sbt – stibnite, sfs – sufosalts, ga – galena, sph – sphalerite, bour – bournonite, ttd – tetrahedrite, qtz – quartz, carb – carbonates, rt – rutile, ber – berthierite, ccp – chalcopyrite. Explanations: ▢ – abundant mineral, □ – uncommon min- erals, * - other uncommon minerals (abbreviation given in the appropriate row).*

Locality/sample	py	asp	Au	sbt	sfs	ga	sph	bour	ttd	*	qtz	carb	rt	As	Cu	Pb	Sb	Zn	Ag	Au	Au*	sample
dumps of adit 6																						
	■	■									■	■										V/2
	■	■	□	■	■			□				□	□									V/3
	■	■			□							□	□									V/4
	■	□	□								■			0,08	0,001	0,008	0,0014	tr	0,8	2,94	2,97	V-5
dumps of adit 2, left bank of the creek																						
	■	□									■			0,06	0,030	0,370	0,244	0,005	9,6	7,66	7,50	V-1
	■	□	□		■						■	■		0,06	0,040	0,167	0,076	0,006	8,4	6,00	6,02	V-6
	■	□			□						■			0,43	0,002	0,127	0,130	0,005	5,2	11,40	11,78	V-7
	■				■		□				■		□									V-8
	■				■						■	■		0,01	0,003	0,091	0,120	0,007	3,2	1,68	1,60	V-9
dumps of adit 4																						
	■	■			□						■	□	■	0,20	0,001	0,009	1,080	0,006	0,4	7,32	7,20	V-10
	■	■	□	□							■		□									V-11
	■			■							■											V-12
	■										■			tr	0,002	0,018	0,028	0,009	tr	0,10		V-13
	■		□	■	□						■	□	□	0,19	0,020	0,020	0,055	0,008	8,0	5,48	5,25	V-15
	□	□									■											V-16
dumps of adit 6																						
	■	■						□	□		■	■										V-17
	□	□			■						□		□									V-17A
	■	□			□						■											V-17B
	□	■			□						■	□	□									V-17C
	□	□			□						■			1,36	tr	0,001	0,020	0,002	tr	8,48	8,42	V-18
	□	■			■						■			2,08	0,001	0,021	0,104	0,003	1,2	9,2	9,40	V-19
	□	□			■						■			0,05	0,001	0,087	0,312	0,003	2,4	9,52	9,96	V-20
	■										■			tr	tr	0,005	0,014	0,001	tr	0,36		V-21
	■				□			□	□		■	■										V-22
	■	■	□		□						■	■		0,21	0,005	0,180	0,170	0,053	2,0	2,12	2,06	V-22A
	■				■			□	□		■	□	□	2,60	0,003	0,038	0,035	0,008	1,6	13,60	14,38	V-22B
dumps of adit 2, right bank of the creek																						
	□	■	□								■	■	□									V-23
	■										■	□										V-23A
	■	□									■	■										V-23D
	□	□		■							■	□		0,07	0,003	0,100	0,115	0,010	1,6	7,44	7,15	V-23E
	■						□				■	■		0,13	0,023	2,080	3,450	0,875	33,6	1,54	1,56	V-24
	□			□			□				■			0,10	0,048	1,850	3,900	0,170	42,0	3,98	3,91	V-25
	□	□		■	■		□				■	■		0,12	0,030	4,690	3,850	1,450	30,8	0,88		V-26
	□				■						■	■	□									V-26A
	■		□		■						■		□									V/26B
	■										■	■	□	0,52	0,005	0,078	0,075	0,020	4,4	5,74	5,49	V-27

Locality/sample	py	asp	Au	sbt	sfs	ga	sph	bour	ttd	*	qtz	carb	rt	As	Cu	Pb	Sb	Zn	Ag	Au	Au*	sample
dumps of adit 1																						
V-28	□										■	■		tr	0,003	0,118	3,600	0,005	1,2	2,34		V-28
V-29	□	□	□	■							■	□		0,32	0,003	0,088	4,100	tr	2,8	6,76	2,45	V-29
V-30	■	□		■	■						■	□		tr	0,001	0,015	0,176	0,003	0,4	0,34	6,54	V-30
V-31	□	□		■						ber	■	■	□	tr	0,001	0,089	0,032	tr	2,0	3,38	3,32	V-31
V-32	■			■	□						■	■	□	0,09								V-32
dumps of adit Vyšná Spodná																						
V-34	■			■	■	□					■											V-34
V-34A	■			■	□	■					■											V-34A
V-35	■					■					■			0,04	0,008	5,060	0,935	tr	39,6	0,62		V-35
V-36	■				□						■			0,04	0,048	6,940	1,110	tr	108,8	0,38		V-36
V-37	□				□						■	□		tr	0,001	0,174	0,134	0,001	2,8	0,12		V-37
dumps of adit Nová Vyšná																						
V-38	□				□						■		□									V-38
V-39	□			■	□						■		□									V-39
V-40	■			■	■		□				■	□										V-40
V-41	■				■		□				■											V-41
V-42	■		□	■	□		■				■											V-42
V-43	■				□	■	■		□		■											V-43
V-44	■				□	□	□				■			tr	0,003	0,555	0,490	0,028	5,6	0,68		V-44
V-45	■				□						■			0,05	0,013	3,190	0,100	0,018	50,8	0,02		V-45
dumps of adits with Fe-Cu mineralization																						
V-46	■				■			□	□		■	□										V-46
V-47	□							■	□		□	■		0,05	0,014	0,132	0,336	0,006	7,6	0,40		V-47
V-48	□										■	■		0,11	0,900	1,600	0,870	0,078	118,4	0,08		V-48
V-48A								■	■					0,10	1,050	2,025	0,630	0,063	126,0	0,26		V-48A
V-49	□								□	ccp	■											V-49
V-50	□								□		■	□										V-50
sample	py	asp	Au	sbt	sfs	ga	sph	bour	ttd	*	qtz	carb	rt	As	Cu	Pb	Sb	Zn	Ag	Au	Au*	sample

Table 13. Correlation matrix of element concentration in bulk samples from Dve Vody.

	As	Cu	Pb	Sb	Zn	Ag	Au
As	1.00						
Cu	-0.23	1.00					
Pb	-0.15	0.58	1.00				
Sb	-0.21	0.42	0.65	1.00			
Zn	-0.12	0.43	0.96	0.58	1.00		
Ag	-0.19	0.81	0.82	0.67	0.71	1.00	
Au	0.66	-0.13	-0.31	-0.25	-0.33	-0.23	1.00

36

temporal relationship between stibnite and sulfosalts. They may represent a product of local action of circulating fluids rather than a general picture of the deposit evolution. A tentative paragenetic relationship of the sphalerite-sulfosalt and stibnite parageneses is indicated in Fig. 9. However, a further detailed study is needed to resolve the question of temporal relationship between stibnite and sulfosalts.

The base-metals mineralization is simple in its mineral composition and was probably formed during a single hydrothermal event. The massive galena-pyrite ores strongly resemble the ores from the deposit Jasenie-Soviansko, situated about 5 km W from the Dve Vody deposit. Luptáková et al. (2000) investigated the ores of the Jasenie-Soviansko deposit and found that a) the silver concentration in galena (analyzed by EMPA) is lower than previously reported, and b) elevated silver concentration could be recorded only in tetrahedrite inclusions. These results are identical as the results for the base-metals mineralization in the Dve Vody deposit and may lead to rethinking of the role of galena in the deposits of the Nizke Tatry Mts as a major silver carrier.

Mineralizations rich in copper sulfides and variable amount of siderite are known from many localities in the Nízke Tatry Mts (Ozdín & Chovan, 1999, Ozdín & Pršek, 2000). At the Dve Vody deposit, the abundance of siderite along with copper sulfides links this mineralization unambiguously to the siderite mineralization in the Nízke Tatry Mts.

In summary, the presented work brings new information on mineral and chemical composition of the ores in the Dve Vody deposit. Many minerals, known from the deposit from previous work (mainly Hak, 1966), were analyzed and identified by electron microprobe for the first time here. The information about chemical composition of carbonates and sulfosalts and their successive relations is especially considered interesting. We attempted to identify the principal carriers of gold and silver in the deposit. In terms of mineral and chemical composition, and the sequence of ore deposition, the deposit Dve Vody is similar to other Sb-Au deposits in the Nízke Tatry Mts.

Acknowledgements

References

Bakos F. & Chovan M., 1999: Genetical types of gold from Magurka deposit (Nízke Tatry Mts). Min. Slov., 31, 217-224. (in Slovak)

Bakos F., Chovan M. & Michálek J., 2000: Mineralogy of hydrothermal Sb, Cu, Pb, Zn, As mineralization in NE of the Magurka deposit, Nízke Tatry Mts. Min. Slov., 32, 497-506. (in Slovak)

Biely A. & Bezák V., 1997: Explanations to the geological map of Nízke Tatry Mts. Dionýz Štúr Geol. Inst. (Bratislava). (in Slovak)

Cabri L.J., 1992: The distribution of trace precious metals in minerals and mineral products. Miner. Mag., 56, 289-308.

Cambel B., Jarkovský J., Gerthoferová H., Krištín J. & Streško V., 1976: Contribution to geochemistry of iron and mercury in antimonites of the West Carpathians. Geol. Sborn., 27, 319-329.

Chovan M., (ed.),1993: Mineralogy of the ore vaste dumps on the Au-Sb deposit Magurka. Manuscript, PRIFUK Bratislava, 72. (in Slovak)

Chovan M., Póč I., Jancsy P., Majzlan J. & Krištín J., 1995: Sb-Au (As,Pb) ore mineralization at the Magurka deposit, Nízke Tatry Mts. Min. Slov., 27, 397-406. (in Slovak)

Chovan M., Slavkay M. & Michálek J., 1996: Ore mineralizations of the Ďumbierske Tatry (Western Carpathians, Slovakia). Geol. Carp., 47, 371-382.

Gubač J., 1980: On geochemical prospection for Sb in the Ďumbier zone of the Nízke Tatry Mts. In: J. Ilavský (ed.), Antimony ore mineralizations of Czechoslovakia, Dionýz Štúr Geological Institute (Bratislava), 89-102. (in Slovak)

Hak J., 1966: Mineralogy and geochemistry of the stibnite deposit in the Nízke Tatry Mts. Sbor. Geol. Věd, Ser. TG, 7, 71-131. (in Czech)

Hovorka D., Méres S. & Ivan P., 1994: Pre Alpine Western Carpathians basement complexes: lithology and geodynamic setting. Mitt. Österr. Geol. Gesell., 86, 33-44.

Janák M., Pitoňák P. & Spišiak J., 1993: Banded amphibolic rocks from the Low and Western Tatra Mts.: Evidence of the lower crustal components in the pre-Alpine basement of the Western Carpathians. Geol. Carp., 44, 260.

Kantor J., 1948: Stibnite at the Dve Vody deposit. Manuscript, Dionýz Štúr Geological Institute (Bratislava). (in Czech)

Kantor J. & Rybár M., 1964: Isotopes of lead from several deposits of West Carpathian crystalline. Geol. Sbor. Slov. Akad. Vied, 15, 285-297.

Luptáková J., Chovan M. & Huraiová M., 2000: Pb, Zn, Cu, Sb hydrothermal mineralization at the locality Jasenie-Soviansko (Nizke Tatry Mts). In: Uher et al. (eds.): Mineralogical – petrological symposium Magurka '2000, August 2000, p. 24. (in Slovak)

Majzlan J., 1996: Ore mineralizations in the Mlynná dolina valley. Unpublished B.Sc. thesis, Comenius University (Bratislava). (in Slovak)

Majzlan J., Chovan M. & Michálek J., 1998: Ore bodies at Rišianka and Malé Železné: Mineral composition and parageneses. Min. Slov., 30, 52-59. (in Slovak)

Michálek J., 1993: Metallogenesis and perspectives of Sb mineralizations in the crystalline complex of Ďumbierske Tatry Mts. Min. Slov., 25, 5, 359-361. (in Slovak)

Michálek J., 1999: Geological and metallogenetic characterization of the Au-polysulphidic mineralization of the Dve Vody-Karol deposit in the Ďumbierske Tatry Mountains. Min. Slov., 31, 225-232. (in Slovak)

Moëlo Y., 1982: Contribution a l'étude des conditions naturelles de formation des sulfures complexes d'antimoine et plomb (sulfosels de Sb/Pb); signification métallogenique. Mem. Sci. Terre Univ. Curie, (Paris), 82 pp.

Ozdín D. & Chovan M., 1999: New mineralogical and paragenetic knowledge about siderite veins in the vicinity of Vyšná Boca, Nízke Tatry Mts. Slovak Geol. Mag., 5, 255-271.

Ozdín D. & Pršek J., 2000: Siderite mineralization in the Nízke Tatry Mts., Western Carpathians, Slovakia. Acta Min.-Petr., Supplementum 2000, 82.

Petrík I., Siman P. & Bezák V., 1998: Granitoid protolith of the othogneissses of the Ďumbier part of the Nízke Tatry Mts, distribution of barium in K-feldspar megacrysts. Min. Slov., 30, 265-274. (in Slovak).

Pulec M., Klinec A. & Bezák V., 1983: Geology and prospection of the scheelite-gold mineralization in the area of Kyslá nearby Jasenie (delimitation of the perspective zone). In: J.Pecho (ed.), Scheelite-gold mineralization in the Nízke Tatry Mts. Dionýz Štúr Geological Institute (Bratislava), 11-38. (in Slovak).